1D- and 2D-Sparse-Array-Optimization

P.K. Weber, L.Peter

Fraunhofer Institut Biomedizinische Technik
Ensheimer Straße 48, D-66386 St.Ingbert

A. Austeng, S. Holm.

Department of Informatics, University of Oslo
P.O. Box 1080, N-0316 Oslo

N. Aakvaak

Vingmed Sound AS, Research Department,
Vollsveien 13C, N-1324 Lysaker, Norway

ABSTRACT

3D-ultrasonic imaging can be achieved by steering conventional single-element-scanners (pseudo 3D imaging). The use of 2D arrays offers a wide range of possibilities, which will lead beyond the limitations of pseudo 3D imaging. The introduction to market of a high-end ultrasonic device for real 3D imaging was announced for fall 97. The transducer of this device is a electronically steered and focused 2D sparse array, which uses only a fraction of the channels required for a fully sampled array. The distribution of the reduced number of channels can be optimized by the use of different methods to achieve acceptable properties for the radiation pattern.

An improved genetic algorithm for sparse array optimization will be presented. For a linear array the optimization results according to this algorithm and two other methods have been compared to measurements and were presented in [1]. For a 2D-array the optimization results of the improved algorithm will be presented.

INTRODUCTION

As a basis for volumetric ultrasonic imaging two-dimensional ultrasonic arrays (2D arrays) provide the possibility of three-dimensional (3D) electronic focussing and beam steering. There are several reasons, why 3D ultrasound is one of the ultimate goals in diagnostic imaging. Volumetric imaging without the drawback of the long acquisition time of 2D cuts will be possible as it is of big advantage in fetal diagnosis, urology, angiography or cardiology. Longterm Doppler monitoring is possible without the

problem of loosing the sample volume by implementing a tracking algorithm to the beam former [2]. Compared to mechanical driven linear arrays, no mechanical losses will reduce the performance of the transducer.

To have the full electronical control on 3D focussing and steering the distance between two neighbouring elements (pitch) should be half of the wavelength of the ultrasound in the propagation medium ($\lambda/2$-pitch requirement). For an array with a diameter of 11 mm at a frequency of 3.5 MHz this will lead to 50×50=2500 elements with a pitch of 220μm. Each of these elements should be connected to a transmit-receive channel. Using existing technologies, the fabrication and implementation of arrays with that big number of elements is very difficult and expensive. One possibility to reduce the number of channels is the use of synthetic aperture techniques [3]. A second approach bases on the principle of aperiodic statistical array [4]. The fully sampled or dense array, as it is called when containing all elements, is thinned by randomly removing elements until a given order of reduction is reached. Turnbull et al. have shown that the mainlobe of the radiation pattern is mostly unaffected by the random removal but the avarage sidelobe level increases as the number of channels decreases [5]. As long as using the same array for transmit and receive gratinglobes in the radiation pattern are prevented by avoiding periodicities in the element locations. The resulting thinned array is called 'sparse array of order n' if the number of elements is reduced to 1/n-th of the original set. Avoiding periodicities in the element locations is not valid for the third approach, the Vernier-method. This is possible, because it uses different transmit- and receive arrays, both with sparse but periodic element distributions. The resulting radiation pattern avoids gratinglobes as a result of the convolution of the transmit and receive pattern [6]. This approach is used for the probe of 3D-Ultrasound's "Model 1", the first full elctronical ultrasonic "3D-machine" on the market. By using a genetic algorithm we started our work on 2D-sparse arrays according to the second method several years ago to design a transducer for the longterm Doppler monitoring of neonats [7]. In this paper, we present our recent results obtained for the design and pattern-optimization of a 2D sparse array with aperiodic statistical element distribution for cardiologic applications and compare it to results according to the Vernier method. This work was partly sponsored by the ESPRIT program of the European Union under contract EP 22982 (NICE-project).

METHOD

From a given dense 2D array with k elements the number s of sparse arrays of order n that can be obtained by random choice is

$$s = \binom{k}{r} = \frac{k!}{r!\,(\mathrm{k}-\mathrm{r})!},\ r = \frac{k}{n}$$

For a 2D-array with 1936 elements and a reduction down to order 8 as it is requiered in our case of designing a transducer for cardiological diagnosis this will lead

to a number of $s = 1.7 \cdot 10^{315}$ possibilities. The question that arises with this huge number of different element distributions is whether there is one of them with better sound field characteristics than others. There is no closed or unified theory that tells us, whether this best one exists and how to find it. And it is absolutely impossible to test all these configurations.

Several search-strategies (optimization algorithms) have been implemented to optimitze the layout of sparse arrays. We have implemented a genetic algorithm basing on the principles of evolution to find probably not the best but a good solution. The overall criterion that controls our optimization algorithm is to come as close to the imaging quality of the dense array as possible. According to that ‘optimized layout‘ means distributing the elements in a way to minimize the differenc of the radiation patterns of the dense and the sparse array.

To obtain a good imaging quality there are three requirements on the radiation pattern of the array that are controlled by the element distribution:

1. Small beamwidth of the mainlobe and low first sidelobes which results in high lateral resolution.
2. Avoiding peaks in the sidelobes of higher order to avoid regions with poor image quality.
3. Keeping good control of steering and focussing.

Figure 1 shows how the radiation pattern (beam pattern) of a 2D-array is represented. To get the full two-dimensional properties of the pattern, the pressure distribution on the halfsphere for $z \geq 0$ is computed. There are two main approaches to do this:

The first one, which is used by our group, is according to Huygen’s principle. The surface of the 2D array (aperture) is covered with point-sources. Each of them transmitts a spherical wave into the halfspace above the array ($z \geq 0$). At a point on the sphere the total pressure is computed by superimposing the contributions of all sources. To get the one way radiation pattern the normalized pressure distribution is computed as a function of a mesh of points representing the sphere. Normalization is done to the maximum value of the pressure. To obtain the two way radiation pattern each point of the mesh is treated as a point reflector that sends the received wave back to the array. The two way radiation pattern is the representation of the normalized magnitude of the pressure that is received by the array as a function of the point mesh. In both cases the pattern can be computed for continious wave (cw) or pulsed wave (pw) on a sphere with arbitrary radius..

The second approach uses the far-field approximation and represents the radiation pattern as the spatial Fourier-Transform of the pressure distribution of the aperture. Compared to the first method the advantage is in the possibility of using Fast-Fourrier-Transform-algorithms which leads to a vast reduction in computation time. The two way radiation pattern is obtained by mutliplying the Fourier-Transforms of the transmit and the receive aperture. The disadvantage is that no nearfield properties of the radiation pattern can be taken into account.

Figure 2 shows the element distribution and the two way radiation pattern at R = 40mm for the 2D dense array specified above. The edges of the elements where cut, so that a piston like transducer is obtained. This reduces the number of elements from 2500 to 1936. The radiation pattern is given as a contour plot. The uv-coordinates can be derived from figure 1b. It is according to the projection of the pressure distribution into the xy-plane when looking from positive z-direction towards the origin of the coordinate-system.

IMPLEMENTATION

For a random sparse array of order 8 with 250 elements the radiation pattern and element distribution are given in figure 3. Comparing the two radiation patterns of figure 2b and 3b one can see what influence the thinning of the elements has. There is an increase in sidelobe level and the mainlobe becomes wider. A better view of the differences between the two patterns can be obtained by comparing the radiation pattern on an azimuthal line (Θ=0 and Φ varies from Φ_1 to Φ_2 with $\Phi_2>\Phi_1$) as it is shown in figure 1a. Both azimuthal pressure distributions in the farfield are given in figure 4. For the three properties mentioned above in this case we obtain:

1. There is an increase in –6dB width of the mainlobe from 2.42° of the dense array to 3.24° of the random sparse array. The level of the first sidelobe increases from –35dB to –19dB.
2. Beyond the first sidelobe region the peak level increase from –46dB up to –19dB.
3. Steering and focussing for the sparse array is disturbed by the non even and clustered element distribution.

Because the width of the mainlobe and the level of the first sidelobe are determined by the ratio of the diameter D of the apertur to the wavelength λ of the ultrasound in the propagation medium the first requirement to an optimization-algorithm is keeping the ‘effective diameter‘. As can be seen from figure 3 this was not done for the random sparse array. The peak sidelobe level and the ability of steering and focussing are controlled by the element layout, i.e. how the remaining elements of the sparse array are distributed over the area of the dense array (effective area). As long as not using different arrays for transmit and receive periodicities in the element locations should be avoided and they should cover the whole area as even as possible.

Common to all sparse array optimization methods except those combining different periodic transmit and receive arrays is the evaluation of the quality according to these three requirements. Usually the quality is measured by a fitness-function and the mathematical task of the optimization process is to find its minimum. A good overview on different optimization methods and resulting beam patterns is given in [1] and [8]. Compared to other methods using genetic algorithms in optimization provide good results in short CPU-time [9].

In the case of sparse array optimization we implemented an algorithm based on the principles of evolution according to the following steps: 1. initialization, 2. selection, 3. crossing over and 4. mutation. The method will be presented for a sparse array of order 8 derived from the array of figure 2a with 1936 elements at a frequency of 3.5MHz. The distance between two neighbouring elements is 220µm (λ/2-pitch). Starting from the dense array a set of t=20 sparse arrays of order n=8 were generated by a random choice of 250 elements out of 1936 (initialization). This first set is called the first generation of size t. For each single array of that generation the fitness-function Q was calculated according to the following procedure:

$$Q = k_1 \cdot F + k_2 \cdot W$$

$$W = \sum_{m=1}^{v} \frac{|w_o - w_k|}{w_0}$$

$$F = \sum_{\mathrm{m}=1}^{\mathrm{v}} \sum_{i=1}^{N} [\, p_0(r_i) - p_k(r_i) \,]^2$$

F is called the error energy. $p_0(r_i)$ is the normalized pressure amplitude of the dense array at a point r_i on the uv-sphere, $p_k(r_i)$ is the normalized pressure amplitude of the k-th sparse array. The pressures are computed according to Huygen's Principle for cw-operation. v indicates the number of steering angles and/or focal depths, i.e. the error energy can be calculated for different steering and focussing configurations. The same applies to W which is the absolute value of the normalized difference between the beamwidths of the main lobes of the dense (w_0) and the k-th sparse array (w_k). k_1 and k_2 are factors that weight the influence of the error energy or the beamwidth to the quality factor. Selection was performed by ranking the arrays of the first generation according to their value of Q. The best array was that with the smallest Q-value. A new set of t=20 sparse arrays was generated as the next generation by using the following procedure: The first five arrays of the first generation were copied to that new set without any changes. These five arrays are called parents. For each of them a counter was increased by 1 representing their lifespan. Six new arrays were generated by crossing over. They are called childrens and replace the last six of the previous generation. Crossing over was performed by combining the element pattern of subareas of three of the parents. The choice of the parents and the choice and size of their subareas was controlled by a random function. The remaining 9 were mutated by randomly activating and deactivating single elements of the corresponding arrays of the previous generation. They are called mutants. The number of mutations was controlled by the mutation rate which gives the maximum number of mutated elements for each array. During the whole process an overall procedure controls the number of elements of each array to be 250 as required. After the new generation was completed, the process restarts by selection and the next set was generated by the same procedure desbribed above. The algorithm continued until a given number of generations was reached or until Q falled short of a given value. If the

lifespan of an array reached a maximum, this array was not allowed to contribute to the next generation and it was replaced by an additional children. In our algorithm all given sizes, numbers and values are parameters so that different combinations could be tested.

RESULTS

For the 2D-array of figure 2a figure 5 shows the radiation pattern of the optimized array after 400 generations together with that of the dense array. Compared to the random array the beamwidth of the mainlobe decreases from 3.24° to 2.43°. The first sidelobe has a level of −37dB and the peak level of the higher order sidelobes −39dB. Figure 6 shows the element distributions of the random and the optimized array and a comparison of the azimuthal radiation patterns of both. The elements of the optimized array cover the whole area more even and keep the effective width of the aperture. This was additionally achieved by performing the optimization for three different steering angles ((Θ, Φ)=(0°, 0°), (30°, 15°) and (0°, 30) according to figure 1b). The optimization was done by using the following parameters: t=20, 5 parents, 6 children, 9 mutants, mutation rate=25, lifespan=10. From figure 6 the improvement of the radiation pattern by optimization can be seen very clearly. Measurements that shows the optimization effect to the imaging quality of the array will be performed as part of the NICE-project in 1999. The use of the method for the optimization of 1D arrays and its verification by measurements has been presented in [1].

COMPARISON TO THE VERNIER METHOD

Several different methods for sparse array optimization have been proposed and they can be devided mainly into two approaches [8]. The first one uses the same array pattern for transmit and reveice and the second one allows both to be different. To avoid high sidelobe level the first approach requires nonperiodic element distribution. In the second there is some more freedom because periodic thinning patterns are allowed on both receive and transmit. Based on the effective aperture aproach the desired two way radiation pattern can be obtained by letting the transmit zeros cancel the receive grating lobes and vice versa. Lockwood and Foster used the Vernier method to design a sparse 2D-array according to that method [6]. The receiver is set up as a periodic array with element spacing p×d and the transmitter as a periodic array with (p-1)×d where p is an integer and d is the element spacing. For p=3 and d=λ/2 at 3.5MHz figure 7 shows the element distribution and the radiation pattern of the Vernier-array. The transmitter has 253 and the receiver 241 elements. Both share 29 elements. The complete array contains 465 elements. Although this is more than the 250 of the otimized array presented above the pattern of both are compared in figure 7c. The Vernier array has a −6dB beam width of 2.6° and the first sidelobe has a level of −32dB. The peak sidelobe level outside the first side lobe is −37.3dB. Compared to our approach the results seems to be worse. But

transfering the radiation pattern of both approaches to the imaging quality that can be expected this statement must be modified. Although the first sidelobe level of the Vernier array is higher, the level of the lobes between 5° and 30° are lower.

In diagnostic imaging ultrasonic transducers are driven with pulsed waves (pw). Compared to cw-operation this will reduce the influence of the lobes above 30°. So the influence of the lobes beyond 30° becomes more important for the contrast and the resolution of the image. Figure 8 shows the pw-radiation patterns of the two arrays driven with 3-cycles-burst at a center frequency of 3.5MHz. As can be seen, the sidelobe level of the Verneir array is approximately 15dB lower than that of the optimized array. Future measurements will show how strong this will affect the image quality.

SOME WORDS ABOUT THE BEST SOLUTION - OUTLOOK

One question arises when using genetic algorithms for optimization tasks*: Is the solution found the best and the only one?* From our experience we have to answer*: No!* And that is the answer one would expect when thinking above all the excellent solutions mother nature found by evolution. When running our optimization algorithm five times with the same parameters we obtain five different element distributions. But the properties of the radiation pattern of the corresponding arrays hardly differ. This can be due to the strong effect of the crossing-over-operation that cuts down the number of configurations considered to a small group. One of our future investigations will be to overcome this drawback by improving the implementation of mutation.

A lot of work has been done on the mathematical background of genetic algorithms and evolution strategies and a lot of different implementation strategies were reported [10]. In our group, we successfully use genetic algorithms together with the finite-element-method to improve the mechanical and electrical behaviour of ultrasonic transducers [11]. But noone can tell you whether the method gives you the best solution to your problem. In sparse array-optimization the only way to find it out would be to test and compare all the possibilities that exist for a given order of reduction. But as described under METHODS, the number of possibilities is too huge to perform that search.

As part of the NICE-project sponsered by the EC, measurements will be performed in the next few months to verify our results and to compare it to the Vernier array.

REFERENCES

1. A. Austeng, S. Holm, P.K. Weber, N. Aakvaag, "Imaging Performance of 1D Algorithmically Optimized Sparse Arrays", in Proc. IEEE Symp. Ultrasonics, 1997, pp. 1503-1506.

2. B. Zernikowski, E. Michel, J. Steck, G. Kohlmann, "Cyclic variation pattern of cerebral blood flow velocity and postconceptional age" in Europ. Journ. of Pediatrics, 153, 1994, pp751-755

3. S.W. Smith, G.E. Trahey, O.T. von Ramm, "Two Dimensional Arrays for Medical Ultrasound" in Ultrasonic Imaging, 14, 1992, pp. 213-233.

4. B.D. Steinberg, Principles of Aperture and Array System Design**,** John Wiley & Sons, New York, 1976.

5. D.H. Turnbull, F.S. Foster, "Beam Steering with Pulsed Two Dimensional Transducer Arrays" in UFFC, 38, 1991, pp. 320-333.

6. G.R. Lockwood, F.S. Foster, "Optimizing the Radiation Pattern of Sparse Periodic Two-Dimensional Arrays" in UFFC, 43, 1996, pp.15-19.

7. P.K. Weber, R.M. Schmitt, B.D. Tylkowski, J. Steck, "Optimization of Random Sparse 2D-Transducer Arrays for 3D Electronic Steering and Focusing", in Proc. IEEE Symp. Ultrasonics, 1994, pp. 1503-1506.

8. S. Holm, Bjornar Elgetun, Geir Dahl, "Properties of the Beampattern of Weight- and Layout-Optimized Sparse Arrays", in UFFC, 44, 1997, pp. 983-991

9. T. Bluemecke, "Optimierungsverfahren in der Gegenueberstelleung", in c't, 12, 230, 1991.

10. D.E. Goldberg, Genetic Algorithms in Search, Optimization, and Machine Learning, Addison-Wesley, Nwe York 1989.

11. D. Schmitt, P.K. Weber, "Optimierung piezoelektrischer Ultraschall-Sensoren" in Proc. CADFEM-User-Meeting 1997, pp. 1-17, Fulda 1997.

FIGURES

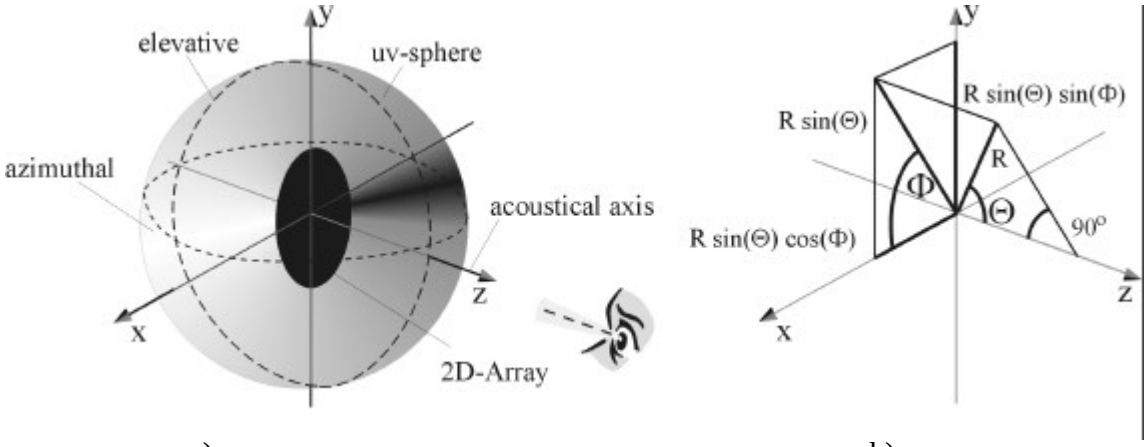

a) b)

Figure 1: configuration for the computation of the radiation pattern
a) the uv-sphere which is located around the array
b) the coordinates related to locations on the sphere

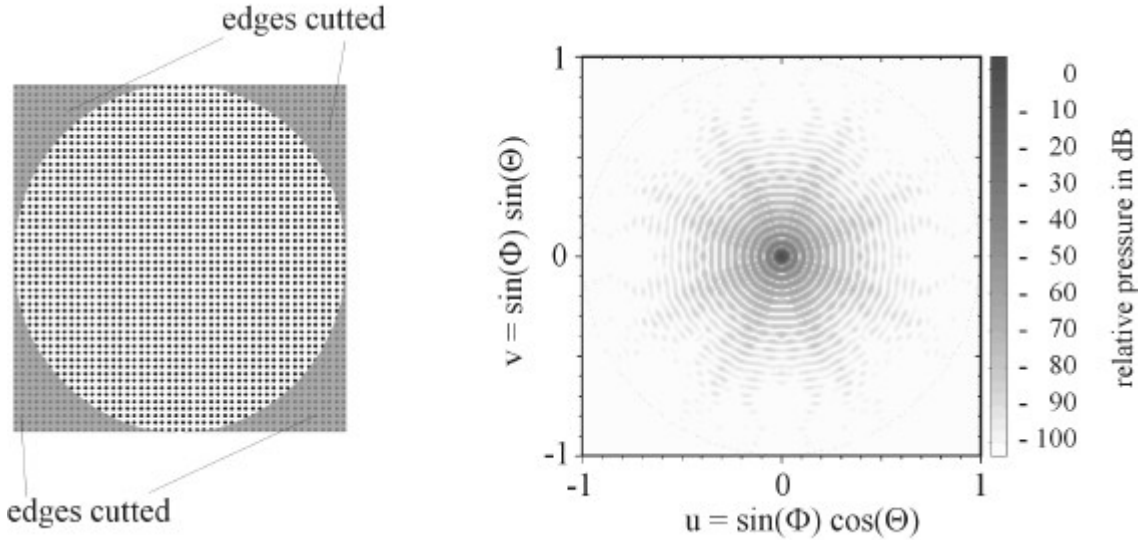

a) b)

Figure 2: element distribution and radiation pattern of the dense array
a) element distribution of 50×50 with cutted edges
b) two-way-radiation pattern on uv-sphere

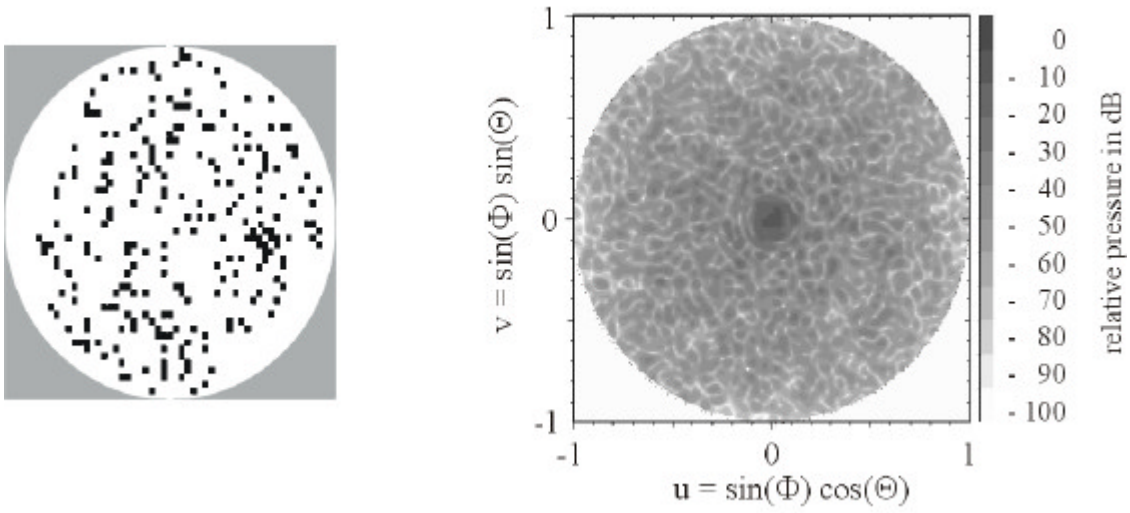

a) b)

Figure 3: element distribution and radiation pattern of a random sparse array of order 8
a) random element distribution
b) two-way-radiation pattern on uv-sphere

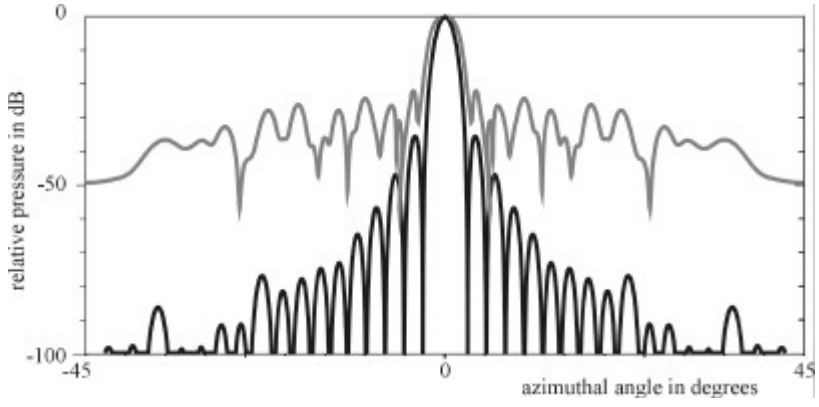

Figure 4: farfield azimuthal radiation patterns of the two arrays of fig 2a and 3a
light grey: random sparse array of fig. 3a
black: dense array of figure 2a

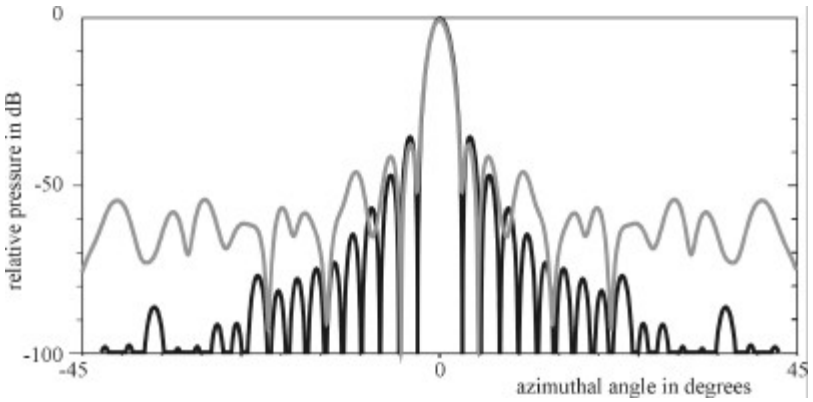

Figure 5: farfield azimuthal radiation patterns of the dense and the optimized sparse array
light grey: optimized sparse array
black: dense array of figure 2a

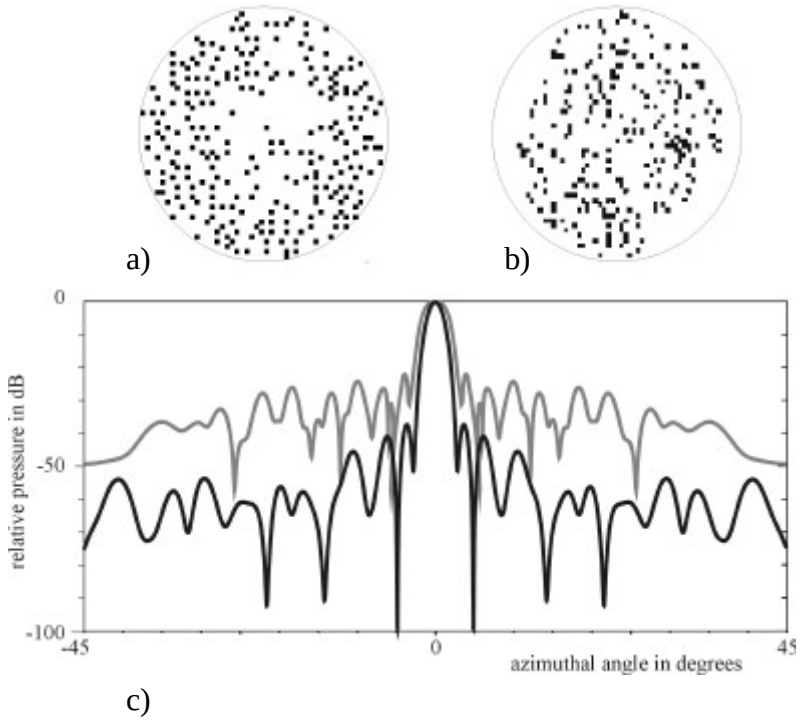

Figure 6: element distributions a) random array, b) optimized sparse array
c) farfield azimuthal radiation patterns, light grey: random sparse array,
black: optimized sparse array

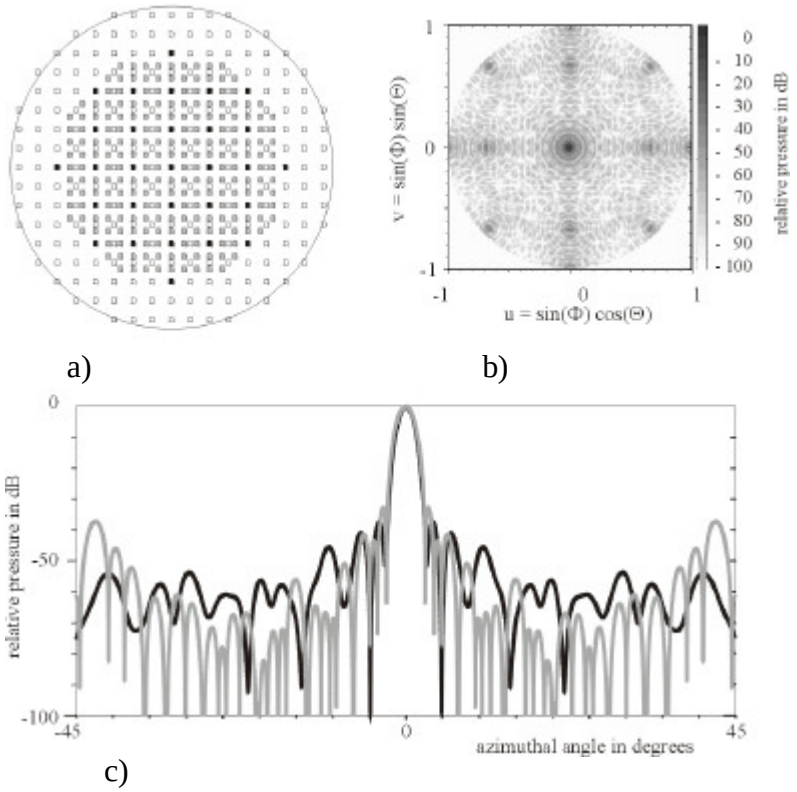

Figure 7: a) element distributions of the Vernier array
(▒ transmitter, □ receiver, ■ common)
b) uv-radiation pattern of the Vernier array
c) farfield azimuthal radiation patterns, light grey: Vernier array, black: optimized sparse array of figure 6a

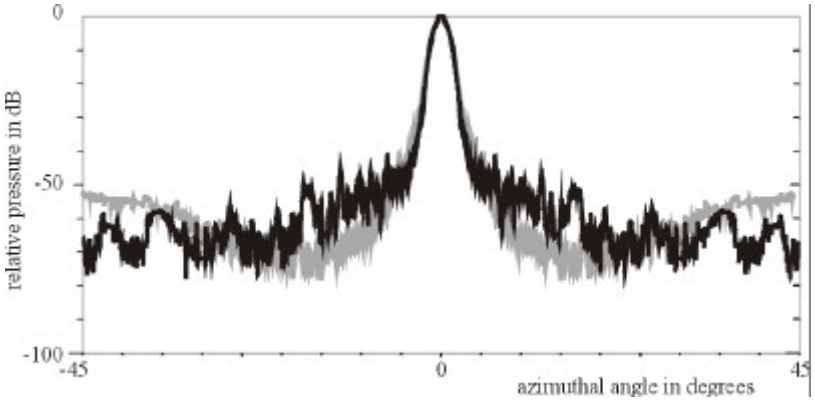

Figure 8: pw-farfield azimuthal radiation patterns of the Vernier and the optimized sparse array
light grey: Vernier array, black: optimized sparse array figure 6a